Journal of Alloys and Compounds 514 (2012) 179–182

Contents lists available at SciVerse ScienceDirect

Journal of Alloys and Compounds

journal homepage: www.elsevier.com/locate/jallcom

Dielectric properties of $CaCu_3Ti_4O_{12}/Pb(Zr_{0.52}Ti_{0.48})O_3$ composite ceramics

A. Rajabtabar-Darvishi [a], W.L. Li [a], O. Sheikhnejad-Bishe [b], L.D. Wang [a], Y. Zhao [a], S.Q. Zhang [a,c], W.D. Fei [a,d,*]

[a] State Key Laboratory of Advanced Welding Production Technology, School of Materials Science and Engineering, Harbin Institute of Technology, Harbin, PR China
[b] Department of Polymer Science and Engineering, School of Chemical Engineering and Technology, Harbin Institute of Technology, Harbin, PR China
[c] Department of Physics, School of Science, Harbin Institute of Technology, Harbin, PR China
[d] School of Machinery Engineering, Qinghai University, Xining 810016, PR China

ARTICLE INFO

Article history:
Received 25 September 2011
Received in revised form 3 November 2011
Accepted 11 November 2011
Available online 25 November 2011

Keywords:
$CaCu_3Ti_4O_{12}/Pb(Zr_{0.52}Ti_{0.48})O_3$ composite ceramics
Dielectric constant
Dielectric loss
Grain boundary

ABSTRACT

A new composite ceramics of $CaCu_3Ti_4O_{12}/Pb(Zr_{0.52}Ti_{0.48})O_3$ have been designed and fabricated to reduce the dielectric loss with certain higher dielectric constant. $Pb(Zr_{0.52}Ti_{0.48})O_3$ was coated on the surface of $CaCu_3Ti_4O_{12}$ particles, and then the composite particles were sintered to obtain $CaCu_3Ti_4O_{12}/Pb(Zr_{0.52}Ti_{0.48})O_3$ composite ceramics using conventional technologies which include the spark plasma sintering. The phase composition and microstructure were studied by means of X-ray diffraction and scanning electron microscopy. The result shows that the ceramics are composed of $CaCu_3Ti_4O_{12}$, $Pb(Zr_{0.52}Ti_{0.48})O_3$ phases (this phase mainly exists at the grain boundary) and some impurities. It is also found that the grain size and the grain shape of composite ceramics are greatly affected by interfacial coating of $Pb(Zr_{0.52}Ti_{0.48})O_3$. The impedance spectrum measurement result shows that the $CaCu_3Ti_4O_{12}/Pb(Zr_{0.52}Ti_{0.48})O_3$ composite ceramics with the $Pb(Zr_{0.52}Ti_{0.48})O_3$ content of 20% has the highest dielectric constant and the lowest dielectric loss.

1. Introduction

Recently, $CaCu_3Ti_4O_{12}$ (CCTO) ceramics [1–4] and doped-CCTO [5–8] have been attracting much attention due to their colossal dielectric constant about 10^5 at room temperature in the frequency range of 100 Hz–1 MHz [9–11]. Furthermore, due to the high dielectric constant, they demonstrate good temperature stability over a range of 100–600 K [5,8,12,13]. So far, the origin of giant dielectric constant of CCTO ceramics has been extensively studied [14–16]. It has also been investigated that the colossal dielectric constant of CCTO is not due to the intrinsic nature of polarization or the ferroelectricity, but it is the result of an extrinsic effect of the barriers [1,5,11]. The interaction of space charge with electrically resistive internal barriers is the most important reason for detecting colossal dielectric constant of CCTO [16]. The study on impedance spectroscopy (IS) of CCTO ceramics has been demonstrated its electrical heterogeneous nature, semiconductor grains and high resistance of boundaries [14]. On the other hand, the internal barrier layer capacitance (IBLC) model has been employed to explain the colossal dielectric constant of CCTO ceramics [4,15]. The dielectric constant depends highly on the material microstructures such as grain size and high resistivity at the grain boundary, which support the IBLC model [6,7,16]. The grain boundary is the main source of internal barrier layer for polycrystalline CCTO ceramics, and hence grain boundary of CCTO ceramics is very important to be characterized [6,7,16].

The main disadvantage of CCTO ceramics is its large dielectric loss. Therefore, studies on the dielectric loss of CCTO have received much attention [1,11,13,17–21]. The small dielectric loss of CCTO ceramics is significant for the device implementation. The relationship between dielectric loss and frequency or temperature has been clearly shown in some researches [1–3,9–11,14,17–22]. From these studies, we can conclude that the dielectric loss of CCTO ceramics is mainly the result of semiconducting grain and grain boundary leakages. Some methods have been explored in order to reduce the current leakages by modifying the semiconducting properties and the interfacial structure of CCTO ceramics [21]. The most important means of changing the intrinsic semiconducting properties of CCTO ceramics is doping. However, doping can decrease the dielectric constant and the dielectric loss of CCTO ceramics [3,6,7,10].

It is very important to investigate the effect of interfacial modification to obtain lower dielectric loss with higher dielectric constant. In the present study, we attempt to use $Pb(Zr_{0.52}Ti_{0.48})O_3$ (PZT) as an interfacial layer to modify the interfacial properties of CCTO ceramics. PZT has been intensively studied, and the results have shown that PZT composition with the Zr/Ti ratio of 52/48 has very high dielectric properties and low leakage current intensity [23]. In this study, PZT was coated on the surface of CCTO powder by sol–gel

* Corresponding author at: Department of Materials Physics and Chemistry, School of Materials Science and Engineering, Harbin Institute of Technology, Harbin 150001, PR China. Tel.: +86 451 8641 3908; fax: +86 451 8641 8647.
E-mail address: wdfei@hit.edu.cn (W.D. Fei).

0925-8388/$ – see front matter © 2011 Elsevier B.V. All rights reserved.
doi:10.1016/j.jallcom.2011.11.052

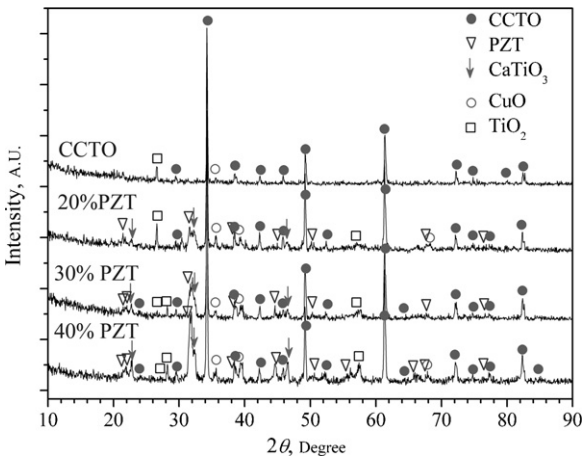

Fig. 1. XRD patterns of CCTO/PZT composite ceramics with different PZT contents.

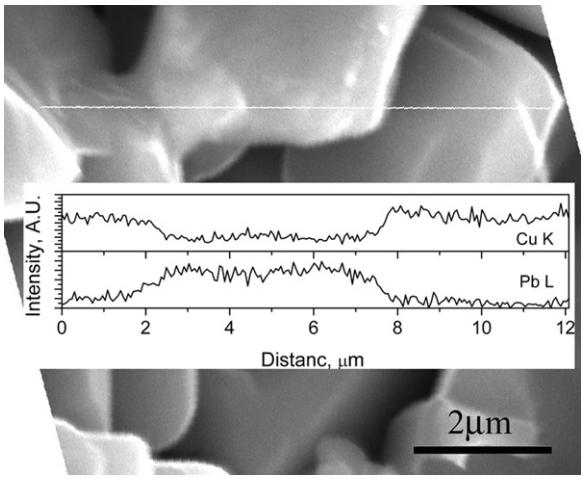

Fig. 2. EDS line scan analysis of Cu and Pb in a typical microstructure of CCTO/PZT composite ceramics with the PZT content of 30%.

method to introduce the interfacial layer of CCTO/PZT composite, and a new CCTO/PZT composite ceramics with low dielectric loss and high dielectric constant was synthesized. In addition, the relationship between the microstructure and properties of CCTO/PZT composite ceramics was also analyzed.

2. Experimental

The CCTO powders used in this study were prepared by sol–gel technology. $Ca(NO_3)_2{\cdot}4H_2O$ (≥99%), $Cu(NO_3)_2{\cdot}3H_2O$ (≥99.5%), $[CH_3(CH_2)_3O]_4Ti$ (98%), and ethylenglycol monomethylether ($C_3H_8O_2$: 95%) as a solvent, were utilized as the starting materials. CCTO sol was dried at 170 °C for 460 min, and then it was sintered at 800 °C for 240 min in air atmosphere to obtain CCTO powder. Finally, the obtained CCTO powders were milled carefully.

PZT precursor with the PZT content of 10 wt% (provided by Mitsubishi Co. Ltd.) was mixed with CCTO powders, and then dried at 200 °C for 10 h. The contents of PZT in CCTO/PZT composite powders were selected in proportion of 20%, 30% and 40% in weight. The powders were milled again and were hot-pressed into the disks with 20 mm in diameter and 4–5 mm in thickness. Subsequently, the CCTO/PZT composite ceramics were sintered using spark plasma sintering (SPS) at 800 °C and 50 MPa for 5 min. Finally, the composite samples were sintered again at 1000 °C for 4 h in the air atmosphere, and were cooled to room temperature in the conventional furnace. However, the required time for common sintering process of CCTO ceramic is generally longer than 20 h [24]. Therefore, to prevent the serious interfacial diffusion, SPS was used to decrease the sintering time in this study.

The relative densities of the obtained composite were measured to be 63%, 85%, 85% and 83% for the PZT contents of 0%, 20%, 30% and 40%, respectively, compared to the theoretical density of pure CCTO [17]. The results suggest that the addition of PZT is helpful for the sintering process of CCTO/PZT composite ceramics.

The phase composition of CCTO/PZT composite ceramics was analyzed by means of X-ray diffraction (XRD) on a Philips X'Pert diffractometer with Cu K_α radiation operated at 40 kV and 40 mA. The microstructure of fracture surface was studied by scanning electron microscopy (SEM) on a Hitachi S-3400N SEM. All the disk ceramics were polished and thinned before IS measurement. The capacitance measurements were carried out as a function of frequency (100 Hz–1 MHz) at 300 K using an impedance gain phase analyzer (Agilent 4294 A) at the signal strength of 0.5 Vrms. For the electrical measurements, the pellets were electroded with room temperature silver agglutinate on both sides, and were dried at 120 °C for 120 min in the furnace.

3. Results and discussion

3.1. Phase composition

The XRD patterns of CCTO/PZT composite ceramics with different PZT contents are shown in Fig. 1. The results show that all samples are well crystallized, and the diffraction peaks of PZT and CCTO can be clearly identified according to the JCPDS files of 75-1149 and 33-0784. As it can be seen in Fig. 1, the positions and intensity of standard peaks of CCTO and PZT are also labeled for each XRD pattern. Using Bragg's law, the lattice constant of CCTO in the composites was calculated using high angle diffraction peak. The result indicates that the lattice constant for all specimens is 0.7394 nm. The obtained lattice parameter for all the samples are in agreement with the values of 0.7391 and 0.7373 nm reported in the previous literatures [1,26]. The mentioned result suggests that the diffusion of PZT into CCTO is not very serious because the lattice constant of CCTO should be changed when Pb and Zr (stand for PZT) are being doped into CCTO.

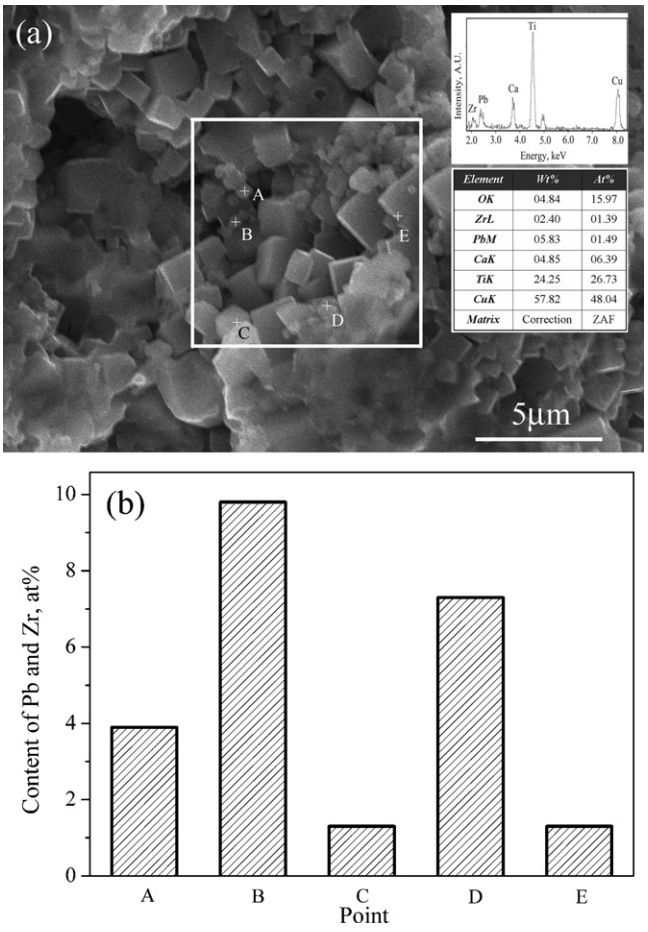

Element	Wt%	At%
OK	04.84	15.97
ZrL	02.40	01.39
PbM	05.83	01.49
CaK	04.85	06.39
TiK	24.25	26.73
CuK	57.82	48.04
Matrix	Correction	ZAF

Fig. 3. EDS analysis of the different points in the CCTO/PZT composite ceramic with the PZT content of 30%: (a) morphology and the insert figures are the average composition of the area marked by white square and (b) Pb and Zr content in the different points shown in (a).

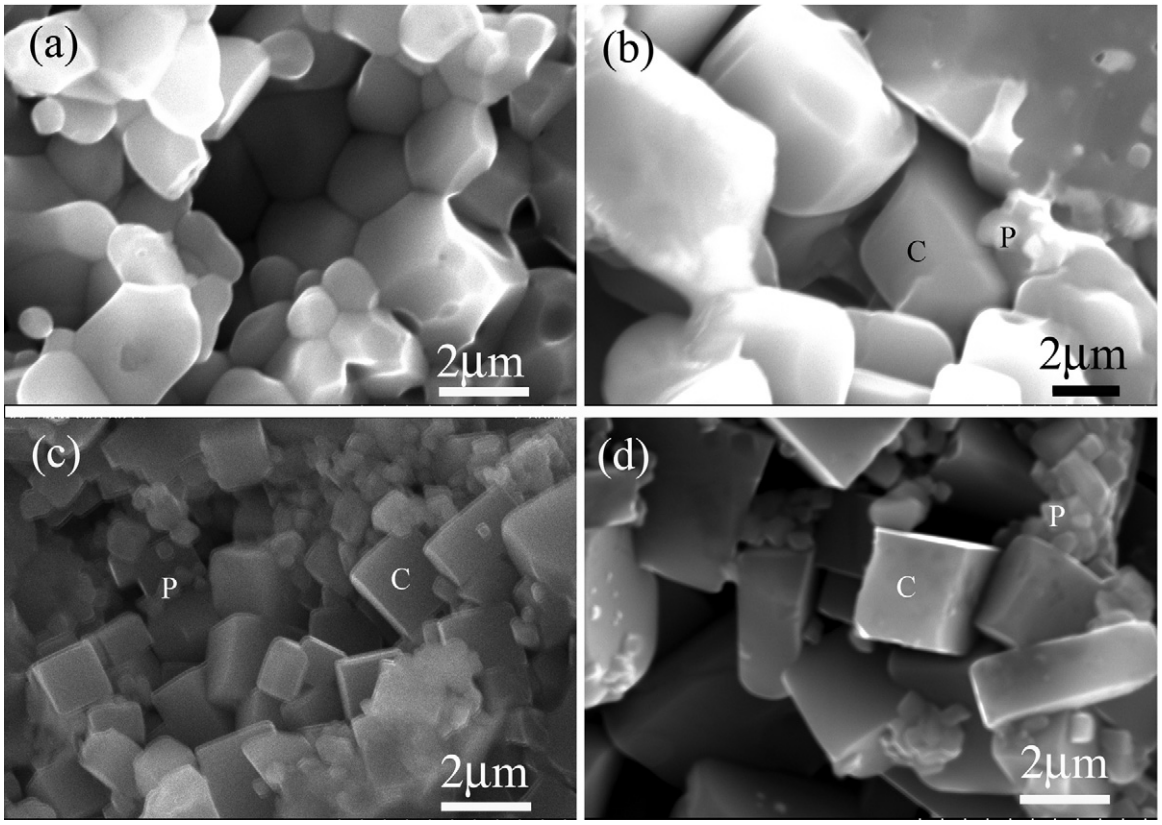

Fig. 4. SEM microstructures of CCTO/PZT composite ceramics with different PZT contents (C: CCTO and P: PZT): (a) 0%, (b) 20%, (c) 30%, and (d) 40%.

On the other hand, as shown in Fig. 1, the diffraction peaks of $CaTiO_3$ (CTO), CuO and TiO_2 can be identified in the XRD patterns of composite ceramics with different PZT contents, which is the result of the decomposition of CCTO phase during sintering process. This result is also in agreement with the results from the previous research [24]. It is worth to mention that the contents of CTO phase are almost the same for all specimens according to the intensity ratios between CTO and CCTO peaks of the composite ceramics. Furthermore, when the PZT content increases, the formation of TiO_2 suppresses and the decomposition of TiO_2 from CCTO decreases.

3.2. Microstructure

Fig. 2 outlines the line distributions of Pb and Cu elements in the CCTO/PZT composite ceramic obtained by the line scan analysis of energy dispersive spectrum (EDS) of SEM. It can be seen that Pb content, which belongs to PZT, is higher in both the grain boundary and the edge of the bigger grain but it is lower in the central part of the bigger grain. The content of CuO in the different CCTO/PZT ceramics is low, and that is difficult to say whether CuO content is decreased or increased with PZT content increasing.

To identify the grains with different shapes, the EDS analysis was carried out point by point corresponding to the morphology, and the results are presented in Fig. 3. As shown in Fig. 3a, the average composition of the area marked by square with white line shows the existence of Pb and Zr on the surface of the sample. As it can be seen in Fig. 3b, Pb and Zr contents at B and D are obviously high for the points in the irregular grain shapes. On the other hand, Pb and Zr contents are very low in the regular grain shapes at points A, C and E. Consequently, the irregular and regular grain shapes might be in association with PZT and CCTO, respectively. However, the light diffusion between CCTO and PZT can be due to the low content of Pb and Zr in the CCTO grains during the sintering process.

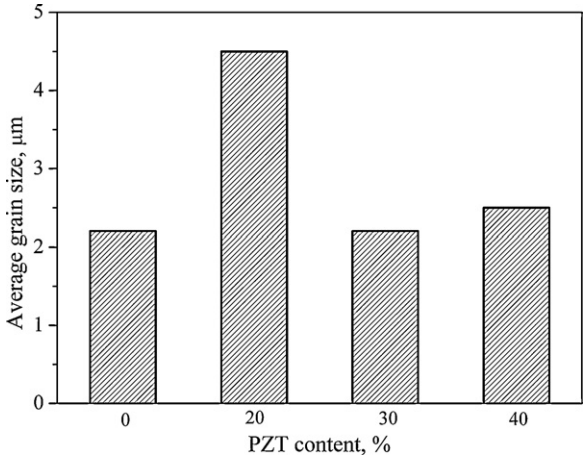

Fig. 5. Average grain size of CCTO/PZT composite ceramics with different PZT contents.

Fig. 4 shows the SEM microstructures of CCTO/PZT composite ceramics with different PZT contents. It can be seen that the grain shapes in pure CCTO are equiaxed while the cuboid-like shapes are regular. The result demonstrates that the growth behavior of CCTO grains changes due to the interfacial coating of PZT. This effect can be caused by the small diffusion of PZT into CCTO grain which changes the surface energy of CCTO particles.

Meanwhile, the grain size of CCTO in the ceramics is also changed greatly. As shown in Fig. 5, the average grain size of the composite ceramic is the maximum for PZT content of 20%. The density measurements of ceramics show that adding the specific amounts of PZT can improve the sintering process. In fact, a small additional PZT is helpful to induce a better contact between

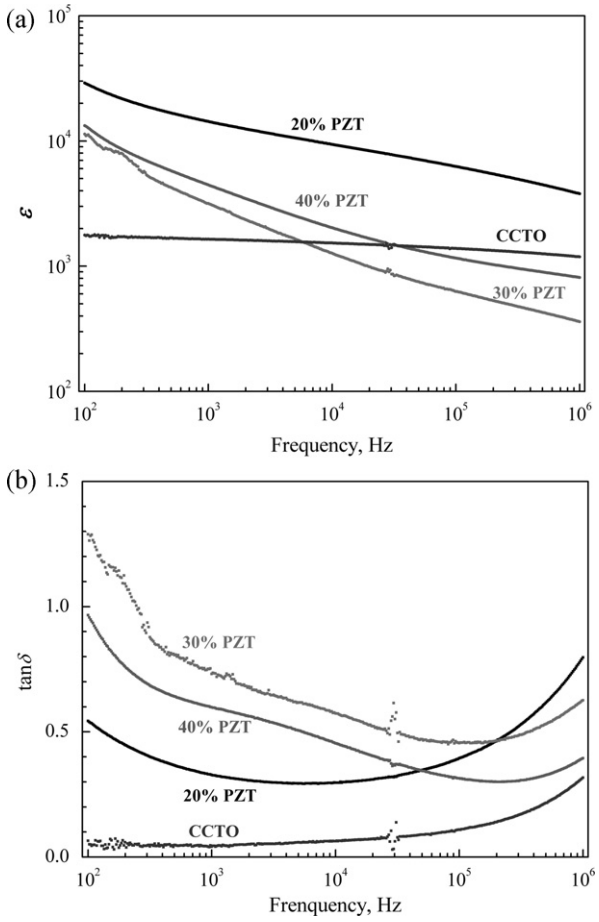

Fig. 6. Comparison of frequency dependences of dielectric properties of CCTO/PZT composite ceramics with different PZT content: (a) dielectric constant and (b) tangent of dielectric loss angle.

the neighbor grains, resulting in the bigger grains and thin interface. The large additional PZT causes a further thickness of the interfaces, and consequently, the contact of CCTO particle would be more restricted, resulting in small grain size of CCTO.

3.3. Dielectric properties

Fig. 6 highlights the variation of the dielectric constant (ε) and dielectric loss (tan δ) versus the frequency. As it can be seen from Fig. 6a, the sample with 20% PZT content has the highest dielectric constant within the whole frequency range selected in this study. The CCTO/PZT ceramics with the PZT contents of 30 and 40% give the same high value of the dielectric constants, as shown in Fig. 6a. The mentioned values are higher than the pure CCTO in the low-frequency range and even lower in the high-frequency range. However, the dielectric constant of pure CCTO ceramic is almost constant through the whole frequency range with a lower ε value. The ε value of pure CCTO in the present study is lower than that has been already reported in the other literatures [13,20–21,25–26]. The only reason to explain the observed effect can be the insufficient density levels of pure CCTO ceramic which causes the high quality CCTO ceramics not to be obtained easily at lower sintering temperature and shorter time.

The dielectric loss of pure CCTO is much lower compared to CCTO/PZT composite ceramics, but its dielectric constant is lower which may be caused by the insufficient compact interface. The dielectric loss of CCTO ceramics is generally high within the high-frequency range [21] which also observed in our study as shown in Fig. 6b. In the lower frequency range, the value of tan δ increases initially with the increase of PZT content, and then it decreases with further increasing of the PZT content.

Compared to the data published in previous literatures [19–22,25,26], our study shows that the CCTO/PZT composite ceramic with the PZT content of 20% has both high dielectric constant and low dielectric loss. According to the above results, it can be concluded that PZT coating of CCTO powder may improve the interface or grain boundary in CCTO/PZT composite ceramics. As shown in Fig. 4, the interfacial layer of CCTO/PZT composite ceramic with the PZT content of 20% is more uniform, and there are small PZT particles on the surface of CCTO grains. In addition, the PZT layer between CCTO grains in the ceramic with the PZT content of 20% should be thinner than that in the ceramics with the higher PZT content. Therefore, the dielectric properties of CCTO/PZT composite ceramic with the PZT content of 20% exhibits higher dielectric properties among the CCTO/PZT composite ceramics.

As shown in Fig. 4c and d, by further increasing the PZT content, the interfacial layer between CCTO grains becomes thicker and some small PZT particles are formed in the composite ceramics. The mentioned phenomenon can reduce the IBLC effect, and it can also enhance the dielectric loss.

4. Conclusions

CCTO/PZT composite ceramics were prepared via the combination of sol–gel, PZT coating of CCTO powders and sintering technology. The PZT phase exists mainly at the interface between the CCTO grains. The grain shape of CCTO is converted into cuboid-like from equiaxed ones with increase in the PZT content. The PZT interfacial coating increases the dielectric constant with an increase of little dielectric loss at suitable coating content. The CCTO/PZT composite ceramics with the PZT content of 20% has the highest dielectric constant and the lowest dielectric loss.

References

[1] A.P. Ramirez, M.A. Subramanian, M. Garrdel, G. Blumborg, D. Li, T. Vogt, S.M. Shapiro, Solid State Commun. 115 (2000) 217.
[2] G. Chiodelli, V. Massarottia, D. Capsonia, M. Binib, C.B. Azzonic, M.C. Mozzatic, P. Lupottod, Solid State Commun. 132 (2004) 241.
[3] B. Zhu, Z. Wang, Y. Zhang, Z. Yu, J. Shi, R. Xiong, Mater. Chem. Phys. 113 (2009) 746–748.
[4] B.S. Prakash, K.B.R. Varma, Physica B 403 (2008) 2246.
[5] T.-T. Fang, W.-J. Lin, C.-Y. Lin, Phys. Rev. B 76 (2007) 045115.
[6] T.-T. Fang, H.-Y. Chung, S.-C. Liou, J. Appl. Phys. 106 (2009) 054106.
[7] F. Luo, J. He, J. Hu, Y.-H. Lin, J. Appl. Phys. 105 (2009) 076104.
[8] B.S. Prakash, K.B.R. Varma, J. Mater. Electron. 17 (2006) 899–907.
[9] M.C. Ferralli, T.B. Adams, A. Feteria, D.C. Sinclair, A.R. West, Appl. Phys. Lett. 89 (2006) 212904.
[10] E.A. Patterson, S. Kwon, C.-C. Huang, D.P. Cann, Appl. Phys. Lett. 87 (2005) 182911.
[11] M.A. Subramanian, D. Li, N. Duan, B.A. Reisner, A.W. Sleight, J. Solid State Chem. 151 (2000) 323.
[12] Y.-S. Shen, B.-S. Chiou, C.-C. Ho, Thin Solid Films 517 (2008) 1209.
[13] A.E. Smith, T.G. Calvarese, A.W. Sleight, M.A. Subramanian, J. Solid State Chem. 182 (2009) 409.
[14] M. Li, A. Feteira, D.C. Sinclair, A.R. West, Appl. Phys. Lett. 88 (2006) 232903.
[15] A.J. Moulson, J.M. Hebert, Electroceramics, Materials, Properties and Applications, second ed., Willey, New York, 2003.
[16] E.A. Paisley, M.D. Losego, S.M. Aygun, H.S. Craft, J.-P. Maria, J. Appl. Phys. 104 (2008) 114110.
[17] R. Mazumder, A. Seal, A. Sen, H.S. Maiti, Ferroelectrics 326 (1) (2005) 103–108.
[18] G. Deng, Z. He, P. Muralt, J. Appl. Phys. 105 (2009) 084106.
[19] J. Zhang, P. Zheng, C.L. Wang, M.L. Zhao, J.C. Li, J.F. Wang, Appl. Phys. Lett. 87 (2005) 142901.
[20] Y. Yan, L. Jin, L. Feng, G. Cao, Mater. Sci. Eng. B 130 (2006) 146.
[21] L. Feng, X. Tang, Y. Yan, X. Chen, Zh. Jiao, G. Cao, Phys. Status Solidi (a) 203 (2006) R22.
[22] T.B. Adams, D.C. Sinclair, A.R. West, Phys. Rev. B 73 (2006) 094124.
[23] J.-K. Yang, W.S. Kim, H.-H. Park, Thin Solid Films 377–378 (2000) 739.
[24] L. Liu, H. Fan, P. Fang, X. Chen, Mater. Res. Bull. 43 (2008) 1800.
[25] M.A. Ramirez, P.R. Bueno, P.R. Tararam, A.A. Cavalheiro, E. Longo, J.A. Varela, J. Phys. D: Appl. Phys. 42 (2009) 185503.
[26] R.N.P. Choudhary, U. Bhunia, J. Mater. Sci. 37 (2002) 5177.